ISSN 1990-7931, Russian Journal of Physical Chemistry B, 2015, Vol. 9, No. 6, pp. 895–900. © Pleiades Publishing, Ltd., 2015.
Original Russian Text © K.A. Avdeev, V.S. Aksenov, A.A. Borisov, S.M. Frolov, F.S. Frolov, I.O. Shamshin, 2015, published in Khimicheskaya Fizika, 2015, Vol. 34, No. 11, pp. 27–32.

COMBUSTION, EXPLOSION, AND SHOCK WAVES

Momentum Transfer from a Shock Wave to a Bubbly Liquid

K. A. Avdeev[a, b], V. S. Aksenov[a, b, c], A. A. Borisov[a, b], S. M. Frolov[a, b, c], F. S. Frolov[a, b], and I. O. Shamshin[a, b, c]

[a] *Semenov Institute of Chemical Physics, Russian Academy of Sciences, Moscow, Russia*
[b] *Center of Pulse Detonation Combustion, Moscow, Russia*
[c] *National Nuclear Research University "MEPhI," Moscow, Russia*
e-mail: smfrol@chph.ras.ru

Received April 3, 2015

Abstract—The transfer of momentum from shock waves of various intensities (from 0.05 to 0.5 MPa) to a water column containing air bubbles of a mean diameter of 2.5 mm is studied both experimentally and by numerical simulation. The experiments are performed in a vertical hydrodynamic shock tube with a rectangular cross section of 50 × 100 mm and a length of 1980 mm. The tube consists of a 495-mm-long high-pressure section, 495-mm-long low-pressure section, and 990-mm-long test section filled with water and equipped with a bubble generator. Experiments have demonstrated that, as the gas content in the water increases from 0 to 30 vol %, the momentum transferred from the shock wave to the bubbly water increases smoothly, leveling off at a volumetric gas content of 20–25%. The experimental and 2D-simulation dependences of the shock wave velocity and the velocity of the bubbly liquid behind the shock wave front on the volumetric gas content are in close agreement.

Keywords: bubbly liquid, shock wave, momentum transfer, experiments, numerical simulations
DOI: 10.1134/S1990793115060032

1. INTRODUCTION

It is known [1, 2] that the thermodynamic cycle with controlled detonation combustion (Zel'dovich cycle) provides a higher thermodynamic efficiency of transformation of chemical energy into the work of expansion as compared to the deflagration combustion at constant volume. Using the Zel'dovich cycle in liquid-fuel rocket engines and air-breathing jet engines has been widely discussed (see, e.g., review [3]), whereas the use of this cycle in hydrojet engines has been discussed only in our papers [4–7]. According to [4–7], a pulse-detonation hydrojet engine consists of a water duct and detonation wave generator operating on a given fuel mixture. The most important problem in the implementation of the Zel'dovich cycle in hydrojet engines is to ensure an efficient transfer of the momentum from the shock wave (SW) coming out from the generator into the water duct to the aquatic medium.

The aim of the present work is to determine, based on experimental and theoretical studies of the interaction of a shock wave with a compressible bubbly liquid, at which the content of gas in the water the momentum transfer from the shock wave to the water is most efficient.

2. LABORATORY SETUP AND THE MEASUREMENT PROCEDURE

Experiments were carried out in a hydrodynamic shock tube (HST) (Fig. 1) with constant rectangular cross-section of 50 × 100 mm^2 and a length of 1980 mm. The tube consisted of a high-pressure section (HPS) of length 495 mm, low-pressure section (LPS) of length 495 mm, test section (TS) of length 990 mm, air bubble generator (ABG), combustible mixture supply system, data acquisition system, and control unit. The pressure in the HPS was measured with a differential piezoceramic pressure sensor (P1 in Fig. 1) and an absolute pressure sensor (P8). The first was used to determine the amplitude of the pressure waves, whereas the second, to measure the initial absolute pressure in the HPS and the pressure in the HPS immediately before the rupture of the diaphragm. The low-pressure section of the HST permanently communicated with the atmosphere through a side opening with a diameter of 3 mm. The basic parameters of the air shock wave formed after the rupture of the diaphragm in the LPS, such as the amplitude, duration and speed of propagation, were determined using two PCB113B24 high-frequency piezoelectric overpressure sensors (P2 and P3). The TS had four optical windows and four PCB113B24 high-frequency piezoelectric pressure sensors (P4–P7). Prior to the experiment, the TS was filled with water. The air bubble generator was placed near the lower end of the TS. The generator was a plate with 152 capillary tubes of inner diameter 0.16 mm, through which air was fed from the receiver into the water in the form of a chain of individual bubbles. The volume fraction of air in the water was determined by monitoring the level of the liquid

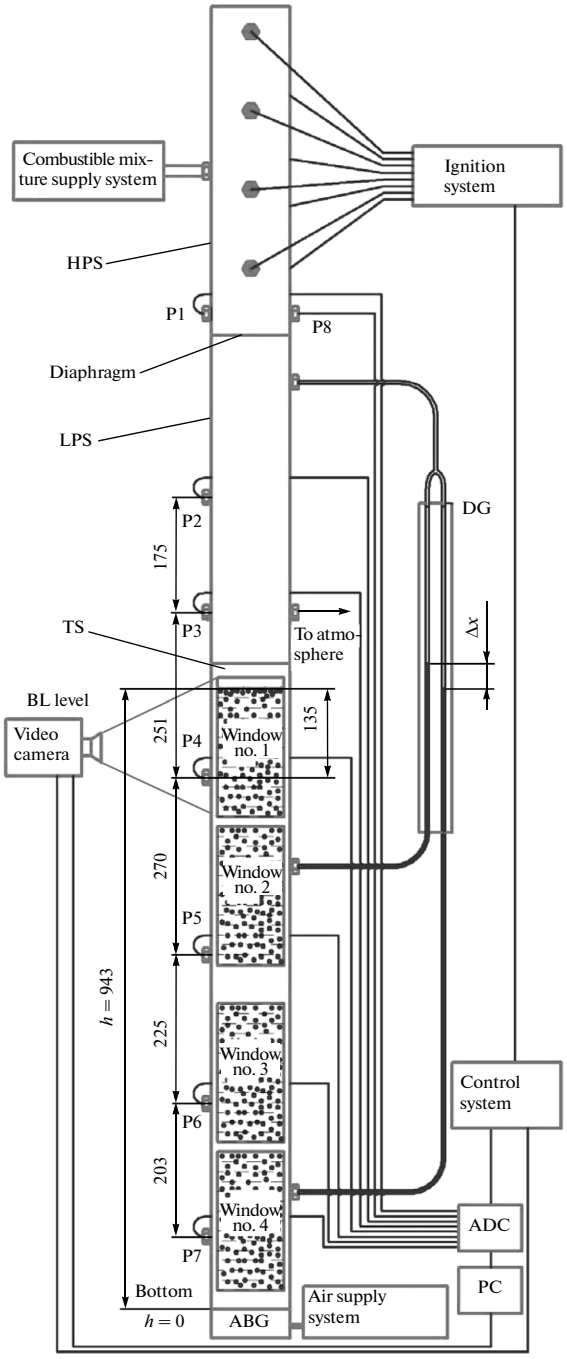

Fig. 1. Schematic diagram of the hydrodynamic shock tube: HPS, high-pressure section; LPS, low-pressure section; TS, test section, ABG, air, bubble generator, DG differential pressure gauge; P1–P7, PCB 113B24 piezoceramic overpressure sensors; P8, Kurant-DA tensoresistive absolute pressure sensor.

(optical window no. 1 with graduation marks) and the level difference in the differential liquid pressure gauge.

The procedure for determining the volume gas content was as follows. Knowing the height of the bubbly medium column h and required initial gas content α_{10}, we determined the equivalent column height of the gas, $h_g = \alpha_{10}h$. Then, the TS was filled with water up to a mark $(h - h_g)$ and air supply was started, with an airflow such as to have the level of the bubbly liquid (BL) set at a mark h. The surface of a bubbly liquid is always covered with a certain number of bubbles that, forming a thin layer of foam, which makes it difficult to establish the exact position of the boundary of the bubbly liquid at high gas content ($\alpha_{10} > 8\%$). Therefore, to more accurately determine the volume of gas content, we used a differential water pressure gauge. Knowing the difference between the heights at which pressure is read ($\Delta h = 496$ mm) and the difference between the heights of the water columns Δx, we can determine the gas content as $\alpha_{10} = (\Delta x/\Delta h) \times 100\%$. The minimum Δx value measurable with the differential pressure gauge to an accuracy of $\pm 0.05\alpha_{10}$ is 10 mm. Thus, the lower limit for the volumetric gas fraction that can be provided by a water pressure gauge is $\alpha_{10} = 2\%$. Smaller values of α_{10} can be obtained only by measuring the height of the liquid column (to within $\pm 0.01\alpha_{10}$).

The table lists the positions of all the pressure sensors relative to the position of the diaphragm of the HST. Since in what follows we discuss primarily the interaction of the SW with the contact surface between the air in the LPS and the bubbly liquid in the TS and the propagation of the SW through this medium, it is convenient to introduce a coordinate system with the origin at the position of the interface at the initial time; i.e., the positions of the pressure sensors in the TS correspond to the depths of their immersion into the bubbly liquid. These coordinates are also given in the table. The times of arrival of the SW front at each particular pressure sensor was determined from the pressure oscillogram, from which and the known lengths of the measuring segments the average velocities of the SW over each segment were calculated. The lengths of the measuring segments are indicated in Fig. 1.

3. MATHEMATICAL MODEL

A detailed description of the mathematical model and numerical procedure for solving the problem of the interaction of a shock wave with a bubbly liquid is given in [5–7]. The mathematical model is based on two-dimensional differential equations of two-phase flow obtained within the concept of interpenetrating continua [8], more specifically, the equations of conservation of mass, momentum, and energy of the phases with additional closure relations describing the dynamic of the interaction of the phases. The system of equations was numerically solved by the SIMPLE method [9], based on the finite volume discretization of the differential equations with first-order approximation in space and time. To avoid excessive refinement of the computational grid near solid surfaces

with no-slip-flow conditions, we used the standard method of wall functions.

4. EXPERIMENTAL AND SIMULATION RESULTS

Experimental studies of the interaction of a SW with a gas-containing liquid were performed for relatively weak and strong shock waves. In the experiments with relatively weak SWs, the diaphragm has a thickness of 25 μm. The pressure in the HPS (≈0.3 MPa at the time of rupture of the diaphragm) was created by supplying compressed air.

In the experiments with strong SWs, the diaphragm thickness was 150 μm, ruptured at a gas pressure in the HPS of ~1.5 MPa, which was created the rapid combustion of a mixture of propane and oxygen-enriched (up to 30 vol %) air. In all the experiments, the LPS was filled with air at atmospheric pressure, whereas the TS was filled with a ≈943-mm-high water column containing air bubbles of average diameter d_{10} = 2.5 mm, with the initial gas content ranging from 0.5 to 30 vol %. The air and water were at room temperature.

As an example, Fig. 2 shows the measured SW velocity in the bubbly liquid over the P5–P6 measuring segment for relatively weak and strong SWs at various initial gas contents α_{10}. The experimental values of the SW velocity were obtained from pressure oscillograms. For comparison, the relevant dependences of the SW velocity on α_{10} calculated by the method described in [5–7] are also displayed.

Distances from the diaphragm to the pressure sensors and the depths of immersion of the sensors (distance from the free surface of the bubbly liquid to the centerline of the sensor)

Sensor	Coordinate, mm	Depth, mm
P1, P8	–32	–
P2	247	–
P3	422	–
P4	673	135
P5	943	405
P6	1168	630
P7	1371	833

The SW velocity was measured over all measuring segments of the TS; in addition, the velocity the contact surface between the air and the bubbly liquid, as well as the speed of individual air bubbles, were measured. The velocity of the contact surface was determined by processing videos from a Phantom Miro LC310 high-speed camera by means of the Phantom Camera Control software. This software enables to measure distances and velocities of selected points after preliminary calibration of the video, i.e., determination of the scaling relation between the image and

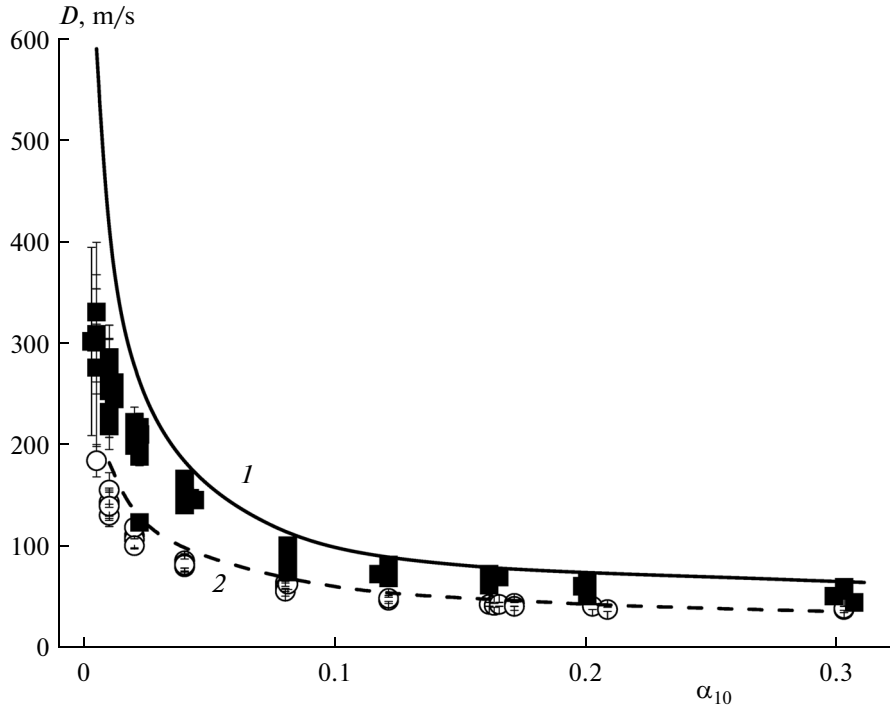

Fig. 2. Dependence of the SW velocity over the P5–P6 measuring segment on the volumetric gas content: (■) strong SW (with an amplitude of ≈0.5 MPa), experiment; (*1*) strong SW (≈0.5 MPa), calculation; (○) weak SW (≈0.05 MPa), experiment; (*2*) weak SW (≈0.05 MPa), calculation.

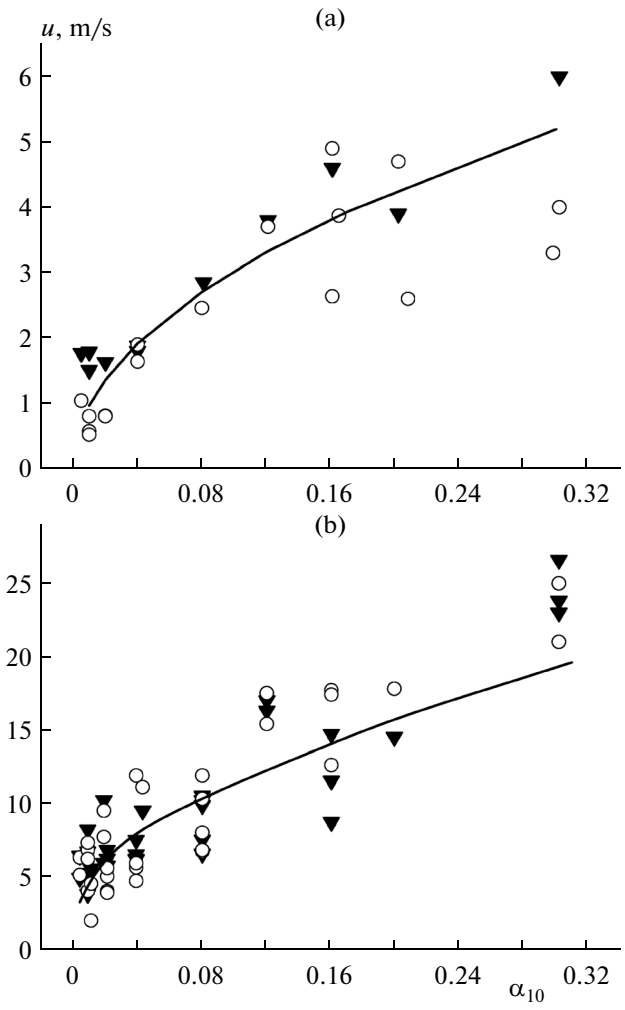

Fig. 3. Comparison of measured (symbols) and calculated (curves) dependences of the contact surface velocity and the velocity of air bubbles u on the initial volumetric gas content for (a) relatively weak (with an amplitude of ≈0.05 MPa) and (b) strong (≈0.5 MPa) SWs: (▼) contact surface velocity and (○) velocity of the bubbles behind the SW front.

the physical object. To do this, the scene always included a scaling segment of known length.

Figure 3 compares the measured and calculated (by the method described in [5–7]) dependences of the velocity of the contact surface and the velocity of air bubbles in the water on the initial volumetric gas contents for SWs of different intensity.

As can be seen from Fig. 3, there is a close qualitative and quantitative correlation between the contact surface velocity and the velocity of the air bubbles behind the SW front. It is also seen that the calculated maximum velocity of the liquid is in good agreement with the experimental data on the velocity of the contact surface and the velocity of the air bubbles behind the SW front throughout the entire range of gas content for relatively weak (Fig. 3a) and for strong shock waves (Fig. 3b).

Based on the measured velocity of the contact surface and the velocity of the air bubbles, it is possible to determine the specific impulse of the liquid behind SW front:

$$I = (1 - \alpha_{01})\rho_2 u_2,$$

where α_{01} is the initial volumetric gas content, ρ_2 is the density of the liquid, u_2 is the velocity of the liquid behind the SW front in the control section or the contact surface velocity, or the bubble velocity behind SW.

Figure 4 compares the measured (symbols) and calculated (curves) dependences of the specific impulse on the volumetric gas content for relatively weak (Fig. 4a) and for strong shock waves (Fig. 4b). As can be seen, the calculated and experimentally determined dependences of the specific impulse are in close agreement over the entire range of volumetric gas contents.

CONCLUSIONS

Systematic experimental and computational studies of transfer of momentum from shock waves with dif-

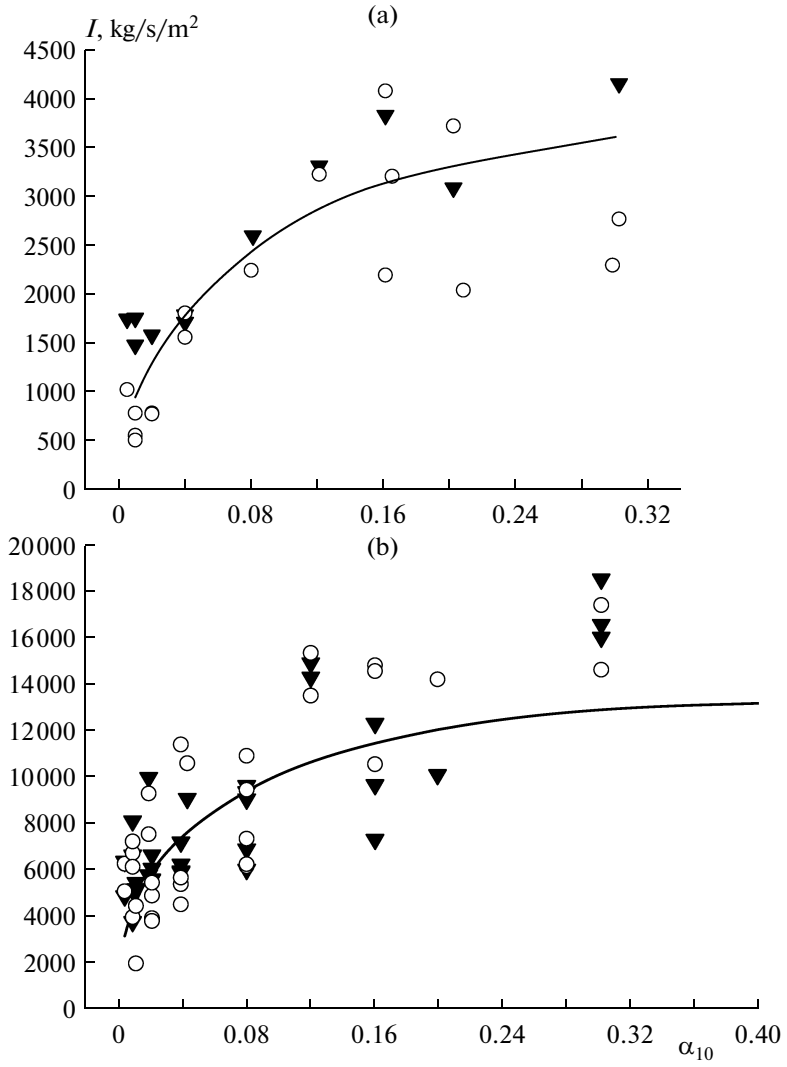

Fig. 4. Comparison of measured (symbols) and calculated (curves) dependences of the specific impulse of the bubbly liquid on the initial volumetric gas content for (a) relatively weak (with an amplitude of 0.05 MPa) and (b) strong (≈0.5 MPa) SWs: the specific impulse of the bubbly liquid is determined from (▼) the measured velocity of the contact surface and (○) the measured velocity of the bubbles.

ferent initial pressure amplitudes (from 0.05 to 0.5 MPa) to an aqueous medium with air bubbles of average diameter 2.5 mm were performed. The experiments were carried out in a vertical hydrodynamic shock tube of rectangular section 50×100 mm^2 with a total length of 1980 mm and lengths of the HPS, LPS, and TS of 495, 495, and 990 mm, respectively. The test section, equipped with a generator of air bubbles, was filled with water. The experiments have shown that, with increasing the gas content from 0 to 30 vol %, the momentum transferred to the bubbly liquid by shock waves increases monotonically, reaching a level at 20–25 vol %. The experimental results were confirmed by two-dimensional calculations of the characteristics of the propagation of shock waves in a bubbly liquid, both for dependences of the shock wave velocity on the volumetric gas content and for the velocity of entrainment of the bubbly liquid in motion.

ACKNOWLEDGMENTS

The authors are grateful to V.A. Smetanyuk for assistance in operating the high-speed video camera.

This work was supported by the Ministry of Education and Science of the Russian Federation under the state contract no. 14.609.21.0001 (contract ID RFMEFI57914X0038) "Development of Technology for Creating Hydrojet Thrust in Water-Jet Engines of High-Speed Water Vehicles and the Construction of a Demonstration Prototype of a Pulse-Detonation Hydrojet Engine" within the framework of the federal target program "Research and Development on Prior-

ity Directions of Scientific-Technological Complex of Russia in 2014–2020."

REFERENCES

1. Ya. B. Zel'dovich, Zh. Eksp. Teor. Fiz. **10**, 543 (1940).
2. S. M. Frolov, in *Pulse Detonation Engines*, Ed. by S. M. Frolov (Torus Press, Moscow, 2006), p. 19 [in Russian].
3. G. D. Roy, S. M. Frolov, A. A. Borisov, and D. W. Netzer, Progress Energy Combust. Sci. **30**, 545 (2004).
4. S. M. Frolov, F. S. Frolov, V. S. Aksenov, and K. A. Avdeev, Request No. PCT/RU2013/001148 (2013). http://www.idgcenter.ru/patentPCT-RU2013-001148.htm
5. K. A. Avdeev, V. S. Aksenov, A. A. Borisov, R. R. Tukhvatullina, S. M. Frolov, and F. S. Frolov, Gorenie i vzryv (Moskva)–*Combustion and Explosion*, 2015, Vol. 8, No. 2, p. 45 [in Russian].
6. K. A. Avdeev, V. S. Aksenov, A. A. Borisov, R. R. Tukhvatullina, S. M. Frolov, and F. S. Frolov, Gorenie i vzryv (Moskva)–*Combustion and Explosion*, 2015, Vol. 8, No. 2, p. 57 [in Russian].
7. K. A. Avdeev, V. S. Aksenov, A. A. Borisov, R. R. Tukhvatullina, S. M. Frolov, and F. S. Frolov, Russ. J. Phys. Chem. B **9**, 363 (2015).
8. R. I. Nigmatulin, *Dynamics of Multiphase Media* (Nauka, Moscow, 1987; Hemisphere, New York, 1990).
9. S. Patankar, *Numerical Heat Transfer and Fluid Flow*, Hemisphere Series on Computational Methods in Mechanics and Thermal Science (Hemisphere, New York, 1980).

Translated by V. Smirnov